Climate regulation of fire emissions and deforestation in equatorial Asia

G. R. van der Werf[a,1], J. Dempewolf[b], S. N. Trigg[c], J. T. Randerson[d], P. S. Kasibhatla[e], L. Giglio[f], D. Murdiyarso[g], W. Peters[h], D. C. Morton[b], G. J. Collatz[i], A. J. Dolman[a], and R. S. DeFries[j]

[a]Faculty of Earth and Life Sciences, VU University, 1081HV Amsterdam, The Netherlands; [b]Department of Geography, University of Maryland, College Park, MD 20742; [c]Integrated Earth System Sciences Institute, Cranfield University, Cranfield MK43 0AL, United Kingdom; [d]Department of Earth System Science, University of California, Irvine, CA 92697; [e]Nicholas School of the Environment, Duke University, Durham NC 27708; [f]Science Systems and Applications, Inc., Lanham, MD 20706; [g]Center for International Forestry Research, Jl. CIFOR, Situgede, Bogor, 16680, Indonesia; [h]Department of Meteorology and Air Quality, Wageningen University and Research Center, 6700AA, Wageningen, The Netherlands; [i]NASA Goddard Space Flight Center, Hydrospheric and Biospheric Sciences Laboratory, Greenbelt, MD 20771; and [j]Department of Ecology, Evolution, and Environmental Biology, Columbia University, New York, NY 10027

Edited by Christopher B. Field, Carnegie Institution of Washington, Stanford, CA, and approved October 27, 2008 (received for review April 8, 2008)

Drainage of peatlands and deforestation have led to large-scale fires in equatorial Asia, affecting regional air quality and global concentrations of greenhouse gases. Here we used several sources of satellite data with biogeochemical and atmospheric modeling to better understand and constrain fire emissions from Indonesia, Malaysia, and Papua New Guinea during 2000–2006. We found that average fire emissions from this region [128 ± 51 (1σ) Tg carbon (C) year^{-1}, $T = 10^{12}$] were comparable to fossil fuel emissions. In Borneo, carbon emissions from fires were highly variable, fluxes during the moderate 2006 El Niño more than 30 times greater than those during the 2000 La Niña (and with a 2000–2006 mean of 74 ± 33 Tg C yr^{-1}). Higher rates of forest loss and larger areas of peatland becoming vulnerable to fire in drought years caused a strong nonlinear relation between drought and fire emissions in southern Borneo. Fire emissions from Sumatra showed a positive linear trend, increasing at a rate of 8 Tg C year^{-2} (approximately doubling during 2000–2006). These results highlight the importance of including deforestation in future climate agreements. They also imply that land manager responses to expected shifts in tropical precipitation may critically determine the strength of climate–carbon cycle feedbacks during the 21st century.

climate change | feedbacks | biomass burning | Indonesia | global carbon cycle

During the Holocene, peat deposits with a thickness of up to 20 m developed in poorly drained areas of equatorial Asia, mostly on the islands of Sumatra and Borneo in Indonesia (1, 2). These peatlands may contain 70 Pg of carbon (3)—a vast reservoir comparable to the carbon stored in aboveground vegetation in the Amazon or ≈9 years of contemporary global fossil fuel emissions. Although these peatlands have accumulated carbon over millennia, the construction of a drainage system to establish rice fields and oil palm plantations has lowered the water table, making the peatlands vulnerable to oxidation and fire (4, 5). Fires are not restricted to peatlands; fire is also extensively used in the forest clearing process and as a management tool in agricultural areas (6, 7).

Fires in Indonesia, Malaysia, and Papua New Guinea have received considerable attention for several reasons, including habitat losses associated with forest conversion (8), the large amounts of carbon combusted (4), and because emissions vary substantially from year to year, contributing to interannual variability of atmospheric CO_2 and CH_4 (9, 10). Total carbon emissions from these fires during the 1997–1998 El Niño were estimated at between 0.8 and 2.6 Pg C (4), equivalent to up to ≈40% of global fossil fuel emissions during that time. Other estimates are lower, but still globally significant, and with large effects on regional air quality (11–13). A decade after the devastating fires of late 1997 and early 1998, the magnitude and dynamics of fires in the region are still not well understood. Also, few emission estimates exist for more recent years, even though rapid forest clearing has probably contributed substantially to the buildup of global atmospheric CO_2. Our main objectives were to quantify fire emissions from the equatorial Asia region during 2000–2006, identify the temporal and spatial variability in fire emissions, and examine the interactions with large-scale forest clearing and peatland draining activities.

Methodology Summary. Our approach relied extensively on satellite data to (*i*) constrain fire emissions from the whole region, (*ii*) calculate annual clearing rates in southern Borneo (where interannual variability in drought was highest), and (*iii*) assess how drought based on precipitation rates from the Tropical Rainfall Measurement Mission (TRMM) (14) affected spatial patterns of fire, especially regarding their distance from drainage canals. Fire emissions estimates were available for 1997–2006 as a subset of the Global Fire Emissions Database version 2 (GFED2) based on burned area (15) and biogeochemical modeling (16) at coarse 1° × 1° resolution. To further constrain these bottom-up estimates—which are uncertain in this region with complex fuel characteristics and uncertain burned area estimates—we transported the GFED2 carbon monoxide (CO) emissions from fires and CO from other sources into the atmosphere, using the GEOS-Chem (17) chemistry transport model. This allowed for a comparison of modeled and measured atmospheric CO column mixing ratios because the latter are measured by the Measurements of Pollution in the Troposphere (MOPITT) (18) satellite sensor (see Fig. 1). We then used the seasonally distinct CO signals from fires in Sumatra and Borneo to optimize the bottom-up emissions from these regions separately so that modeled CO mixing ratios matched measured CO mixing ratios as closely as possible.

After constraining the fire CO emissions for the region in the optimization we assessed the carbon monoxide to carbon (CO:C) ratio of the fires to estimate carbon losses (Fig. 1). CO:C ratios vary between different types of fire, with peat fires emitting up to four times as much CO per unit carbon combusted than other types of fires (19). We combined data of fire activity from the Terra MODerate resolution Imaging Spectroradiometer (MODIS) at 1 × 1 km (20) and land cover classifications including the distribution of peatlands with reported emission factors to assess

Author contributions: G.v.d.W., J. Dempewolf, S.N.T., J.T.R., and R.S.D. designed research; G.v.d.W., J. Dempewolf, S.N.T., P.S.K., L.G., D.M., and W.P. performed research; G.v.d.W., J. Dempewolf, S.N.T., D.C.M., G.J.C., and J. Dolman analyzed data; and G.v.d.W., J. Dempewolf, J.T.R., and R.S.D. wrote the paper.

The authors declare no conflict of interest.

This article is a PNAS Direct Submission.

[1]To whom correspondence should be addressed. E-mail: guido.van.der.werf@falw.vu.nl.

This article contains supporting information online at www.pnas.org/cgi/content/full/0803375105/DCSupplemental.

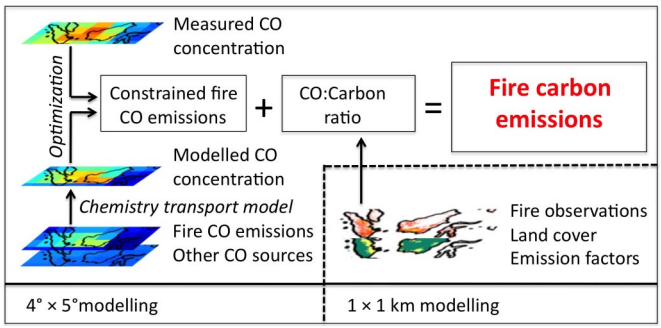

Fig. 1. Schematic overview of the methodology and data sets used to estimate constrained fire carbon emissions. Initial fire CO emissions estimates were available on 1° × 1° resolution while the GEOS-Chem model operated on 4° × 5°, also the resolution to which the measured CO mixing ratios from MOPITT were resampled.

the relative contributions of the different fire types to estimate annual CO:C ratios separately for Sumatra and Borneo. See *Materials and Methods* for more detailed information and for a description of our approach for assessing annual rates of forest loss.

Results and Discussion

Nonlinear Relation Between Drought and Fire Emissions. We found a strong coupling between regional drought intensity and fire emissions. The southern part of Borneo experienced the strongest year-to-year climate fluctuation related to the El Niño—Southern Oscillation (ENSO), leading to large interannual variability in the length of the dry season. Fig. 2 shows how fires mostly occurred during drought years, with very few fires in 2000 when the dry season was short due to La Niña conditions while an extended dry season during the moderate 2002 and 2006 El Niño's led to widespread fires. Although we expected fire activity to increase during drought periods, we found that this relation was strongly nonlinear. Fig. 3 shows how fire activity and emissions in this region increased exponentially with the severity of drought during the dry season. This finding was robust using different data inputs for precipitation rates and fire activity. The nonlinearity also persisted when a longer time window was used to calculate average dry season precipitation, although the correlation coefficients were highest using a 3-month window centered on the driest period each year.

Our finding of a strong nonlinear correlation between fire and climate is of particular concern in the context of future greenhouse gas concentrations and climate change. All of the climate–carbon models analyzed as a part of the Intergovernmental Panel on Climate Change (IPCC) Fourth Assessment report showed a positive feedback between the carbon cycle and the climate system during the 21st century (21). A primary contributing mechanism to this feedback was a reduction of net primary production in the tropics in response to warming and drought (22). The strong nonlinearity between fire emissions and drought described above is likely to further strengthen this positive feedback because increased greenhouse gas concentrations may lead to more frequent or severe drought events (23, 24). Drought, in turn, accelerates forest clearing and emissions from peat fires, further increasing atmospheric greenhouse gas levels in a positive feedback loop. One unique feature of the carbon–climate feedback described here is the human component; because humans set most fires, this mechanism would not exist or would be considerably smaller in the absence of increased human settlement, agricultural expansion, and logging in the region.

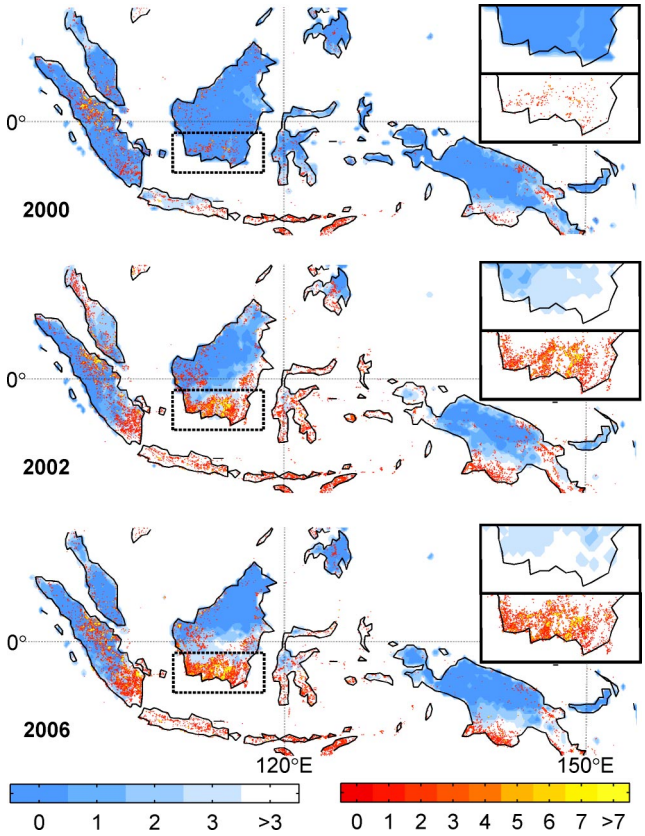

Fig. 2. Dry season length (14) and fire detections (20) for the strong 2000 La Niña and 2002 and 2006 moderate El Niño years. The southern Borneo region is boxed and the dry season length and number of fire detections for this study region are shown in separate insets. The length of the dry season is given as number of months with <100 mm month^{-1} precipitation (Fig. S2, blue-white) and the number of detected fires each year is shown in red–yellow.

Causes of Nonlinearity. Several factors contributed to the nonlinear relationship between climate and fire activity. First, increased drought severity in forests allowed for more rapid clearing rates (Fig. 4) and accidental fires. During the 2002 and 2006 El Niños, for example, forest loss in southern Borneo was 7 and 14 times as high, respectively, as during the 2000 La Niña (Table 1, Fig. 4). During the 2000 La Niña, high rainfall rates year-round may have limited the use of fire by landowners and therefore also the number of fires that escape into nearby forests. Although almost all fires burning in forests were initially set by humans (25), we cannot distinguish between fires set deliberately to clear forest and those that escaped from other land-use types into nearby forests. Second, the average distance of fires to drainage canals increased with drought in the dense network of canals in southeast Borneo [Table 1, supporting information (SI) Fig. S1 in *SI Text*]. This suggests that water table height limited the area where fires could be used as a management tool for forest clearing and where accidental fires escaped during non-drought years. Finally, we found that the number of fires recorded at the same 1-km location on different days during the dry season increased with the severity of the dry season (Table 1). This fire persistence metric is related to fire duration and fuel consumption (26, 27) and indicates that sustained burning in areas with high fuel loads (including peatlands and forests) increased with drought severity.

Positive correlations between drought extent and clearing rates ($R^2 = 0.53, P = 0.06, n = 7$), mean distance of fires to canals ($R^2 = 0.60, P = 0.07, n = 6$), fire persistence ($R^2 = 0.89, P = 0.01, n = 7$), and active fire detections and emissions (see Fig. 3 for

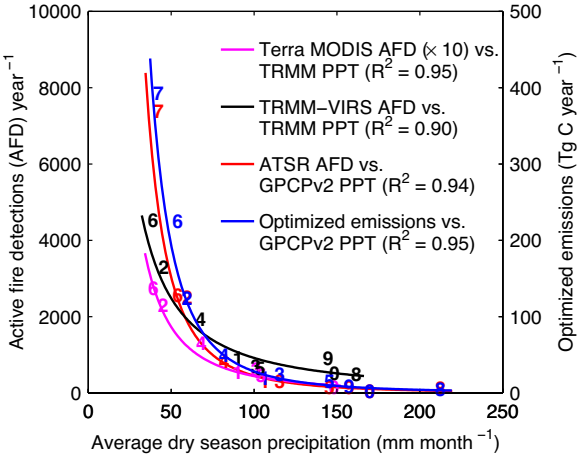

Fig. 3. Relation between average precipitation rates during peak fire season and satellite-derived active fire detections (AFD). Optimized emissions for southern Borneo (south of 1°S), the region most impacted by ENSO-induced interannual variability in precipitation rates, are also shown. Because of variability in the timing of the dry season, here we defined average dry season precipitation as the mean monthly precipitation during the 3 consecutive months with lowest rainfall. The numbers in the graph denote the year (7 = 1997, 0 = 2000, 1 = 2001, etc., through 6 = 2006); correlation coefficients are based on a power fit. Data sources include TRMM (14) and Global Precipitation Climatology Project version 2 (GPCPv2) (36) for precipitation and TRMM-Visible Infrared Scanner (VIRS) (37), (Advanced) Along Track Scanning Radiometer (A)ATSR (38), and Terra-MODIS (20) for active fire detections. Differences in precipitation rates between GPCPv2 (2.5° × 2.5°) and TRMM (0.25° × 0.25°) are caused, in part, by differences in spatial resolution. The large fires in early 1998 in eastern Borneo burned outside this study region.

regression coefficients) imply a strong coupling between climate variability and human land management. The climate sensitivity of these human-mediated losses is not yet accounted for in coupled climate–carbon cycle projections but has the potential to increase the gain of climate–carbon feedbacks (and predicted levels of future warming).

Fire Emissions Estimates. The strong connection between climate and land management led to large interannual variability in emissions; emission estimates from all of Borneo optimized using MOPITT (Table 1) were on average 74 ± 33 Tg C year^{-1} with a minimum in 2000 (7 ± 3 Tg C year^{-1}) and a maximum in 2006 (236 ± 106 Tg C year^{-1}, see Table 1). In Sumatra, fire activity also increased during drought periods but variations in drought conditions from year to year were smaller and droughts were spatially more variable compared to Borneo, both leading to lower interannual variability in Sumatra (coefficient of variation in active fire detections was 0.49 vs. 0.74 for Borneo).

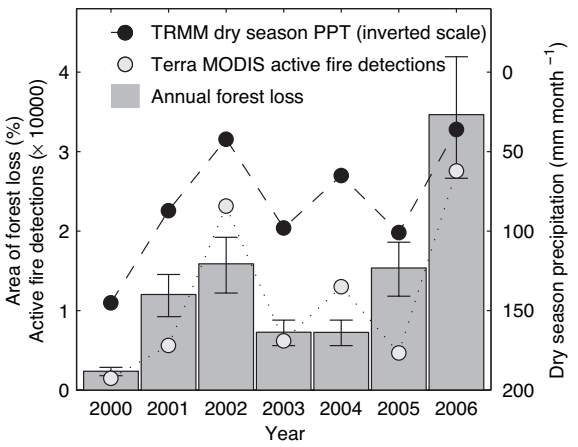

Fig. 4. Interannual rate of forest loss in southern Borneo (south of 1°S) shown as percentage of area with >50% woody cover in 2000 (33), average dry season precipitation based on TRMM precipitation (14), and Terra-MODIS active fire detections (20). Error bars on forest loss rates indicate the omission errors (positive) and commission errors (negative).

Over the 2000–2006 period, an increasing trend in emissions was observed in Sumatra [8 Tg C year^{-2} (= 16% year^{-1} of the 2000–2006 average), $R^2 = 0.61$, $P = 0.02$, $n = 7$]. The drivers of this increasing trend are not well understood and may include an increase in the clearing rate for oil palm plantations (28) or more intense drought during the latter part of our study period. Initial results show that fire activity was low in 2007 in both Borneo and Sumatra due to La Niña conditions (Fig. S3), again illustrating the role of climate in shaping fire conditions and rates of forest loss. MOPITT-optimized emission estimates were not as well constrained in Sumatra compared to Borneo because of the covariance of the fire season with the influx of fossil fuel emissions from mainland Asia. Emission estimates for Sumatra were on average 49 ± 39 Tg C year^{-1}, with a minimum of 23 ± 19 Tg C year^{-1} in 2001 and a maximum of 88 ± 71 Tg C year^{-1} in 2005 (Table 1).

Average emissions over 2000–2006 for the whole region were 128 ± 51 Tg C year^{-1} (Table 1). Most emissions originated from Borneo (58%) and Sumatra (38%). Other contributors included the Indonesian islands of Sulawesi (1%) and Papua (1%), and Papua New Guinea (2%). Interannual variability was large with a minimum during the 2000 La Niña (47 ± 29 Tg C year^{-1}) and a maximum during the moderate 2006 El Niño (303 ± 118 Tg C year^{-1}). Although our estimate of the mean fire flux during 2000–2006 is smaller than several previous estimates (5), it is still comparable to emissions from fossil fuel combustion for the region (fossil emissions were on average 148 Tg C year^{-1} for the sum of Indonesia, Malaysia, and Papua New Guinea during 2000–2004, ref. 29) and highlights the importance of accounting for deforestation fluxes in climate policies designed to stabilize levels of atmospheric CO_2 (30).

To estimate fire emissions for the 1997–1998 El Niño, the strongest El Niño on record, we assumed that the MOPITT-derived optimization scalars to our bottom-up emissions during 2002–2006 were also applicable to bottom-up estimates before the MOPITT era and that the 2000–2006 emission factors were also time independent. This resulted in an estimate for the whole region of 726 ± 228 Tg C year^{-1} for 1997 and 244 ± 95 Tg C year^{-1} for 1998, for a total of 969 ± 248 Tg C during the 1997–1998 El Niño. About 90% (≈870 Tg C) of this estimate originated from Indonesia. Our estimate is thus closer to the lower estimate (810 Tg C) reported (4) than to the often-reported higher estimate (2570 Tg C). Even this lower estimate confirms the important role of fires in the region in explaining part of the high CO_2 and CH_4 growth rates observed during the 1997–1998 El Niño period (4, 9, 10).

Uncertainties. Our satellite-based approach provided constrained estimates of carbon emissions from fires in a region with complicated fuel composition and uncertain burned area estimates. Remaining uncertainties include the amount of carbon lost from forest clearing and peatland drainage that exits the system via decomposition (5). In our analysis approach, uncertainties stem mostly from our approach to estimate CO emission factors and how the lifetime of CO is modeled. Uncertainties in the chemistry-transport model and MOPITT are probably smaller but add to the overall uncertainty.

The relatively good agreement between the optimized model and MOPITT (Fig. 5) indicates that cloud obstruction in the fire detection process is not a major limiting factor. Further con-

Table 1. Annual ENSO index, dry season precipitation, and other parameters affecting fire emissions for Borneo and optimized emission estimates for Borneo, Sumatra, other regions, and all regions combined

		Borneo						Sumatra:	Other regions:	Whole region:
Year	ENSO index* (−)	Dry season precipitation†‡ (mm month^{-1})	Forest clearing rate‡ (% yr^{-1})	Distance to canals§ (km)	Persistent fire fraction¶ (−)	Bottom-up fire emissions‖ (Tg C yr^{-1})	Optimized emissions estimate‖** (Tg C yr^{-1})	optimized emissions estimate‖** (Tg C yr^{-1})	optimized emissions estimate‖** (Tg C yr^{-1})	optimized emissions estimate‖** (Tg C yr^{-1})
2000	−0.21	145	0.24	NA	0.39	8 ± 2	7 ± 3	35 ± 29	4 ± 2	47 ± 29
2001	0.07	87	1.20	0.79	0.52	27 ± 8	27 ± 12	23 ± 19	3 ± 1	53 ± 22
2002	0.73	42	1.59	1.14	0.59	123 ± 35	123 ± 56	46 ± 37	15 ± 7	185 ± 67
2003	0.25	98	0.73	1.03	0.51	28 ± 8	27 ± 12	38 ± 30	2 ± 1	67 ± 33
2004	0.54	65	0.73	1.22	0.54	66 ± 19	66 ± 30	47 ± 38	7 ± 3	120 ± 49
2005	0.35	101	1.54	0.98	0.54	32 ± 9	31 ± 14	88 ± 71	3 ± 2	123 ± 72
2006	0.75	36	3.47	1.48	0.61	234 ± 66	236 ± 106	63 ± 50	3 ± 1	303 ± 118
Mean	*0.35*	*82*	*1.36*	*1.11*	*0.53*	*74 ± 21*	*74 ± 33*	*49 ± 39*	*5 ± 2*	*128 ± 51*

*Dry season (June–October) multivariate ENSO index (MEI, http://www.cdc.noaa.gov/people/klaus.wolter/MEI/mei.html).
†Mean monthly precipitation during the 3 consecutive months with lowest rainfall, based on TRMM precipitation.
‡For Borneo south of 1°S, the region most heavily impacted by ENSO drought. This part of the island had an area of 19 Mha.
§Mean distance to drainage, either canals or rivers, of MODIS active fire observations for a region corresponding to Landsat scene path 118 row 062 in southern Borneo (Fig. S1).
¶Fraction of total detected fires that were detected during more than one satellite overpass in the same 1-km grid cell during the dry season, indicating high fuel loads such as fires associated with forest loss or peat burning that burn for longer periods in the same place (27).
‖Uncertainties represent 1 sigma range.
**Based on the anomaly optimization (see *Materials and Methods*) and the mean of the bottom-up model.

straining emission estimates would require land cover maps at finer spatial and temporal resolution and *in situ* measurements of fuel consumption and emission factors (see *Materials and Methods*). In the absence of such information, our approach based on two scenarios to estimate the partitioning of fires into different land cover types (and thus emission factors) allowed for a partial assessment of error.

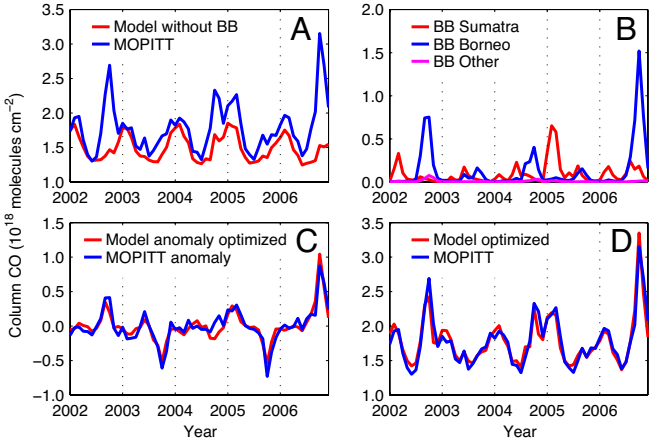

Fig. 5. Comparisons of modeled (Model) and measured (MOPITT) monthly average CO column mixing ratios for a box covering the region 12°N–12°S and 57.5°E–147.5°E. (*a*) Modeled CO from the burning of fossil and biofuel, CH_4 and VOC oxidation, and biomass burning (BB) from regions outside the equatorial Asia region are compared with measured CO, indicating that without fires from equatorial Asia the atmospheric measurements cannot be reproduced. (*b*) CO originating from BB in Sumatra, Borneo, and other regions of equatorial Asia as calculated by our bottom-up model. (*c*) Optimized modeled biomass burning sources and MOPITT anomalies based on a scalar of 0.57 for Sumatra and 1.01 for Borneo, which is used in the main text in combination with the bottom-up modeled mean emissions. (*d*) Optimized sources using scalars for Sumatra fires [0.24] and Borneo fires [1.10], and one scalar for all other sources combined [1.10], and MOPITT measurements (the absolute optimization approach described in *Materials and Methods*).

Conclusions

Satellite observations provided new insight into fire dynamics and carbon losses in this rapidly changing region. The strong nonlinear relation between drought and fire emissions in southern Borneo highlights the sensitivity of the region to climate change and indicates that increased anthropogenic use of fire with drought may be an important positive feedback between climate and the carbon cycle during the 21st century. To date, climate–carbon cycle feedbacks have been mostly modeled as an interaction of canopy-level processes such as reduced net primary productivity and increased soil respiration in response to temperature increases. Our results provide evidence that the response of human agents (land users) to drought may comprise an equally important class of carbon–climate feedback mechanisms in the tropics. Without proper mitigation strategies (30), emissions from this region have the potential to increase substantially as climate projections suggest future drying and warming (23).

Materials and Methods

Emissions Estimate Approach. Fire emissions were constrained in a four-step process. First, we calculated CO emissions on the basis of burned area (15), a biogeochemical model at a 1° × 1° resolution (16), and CO emission factors (31) (Tables S1 and S2). As a second step, we simulated atmospheric CO mixing ratios from fires and other sources and sinks using the GEOS-Chem chemistry transport model (17) at 4° × 5° resolution, separately tracking fire-emitted CO from Borneo, Sumatra, and other regions within equatorial Asia (Fig. 5 *a* and *b*). The resulting atmospheric abundances of CO were compared with satellite CO measurements from the MOPITT sensor (18) (see below, Fig. 5 *a* and *b*, Fig. S4). In the third step we optimized the bottom-up model estimates of CO emissions in two time-independent optimizations, one based on anomalies and one based on absolute values (Fig. 5 *c* and *d*, see below). In the final step, we combined active fires from MODIS (20) with a peatland map (32) and annual fractional tree cover maps (33) at a 1 × 1-km resolution to assess for each year the relative contributions of fires in peatlands, forest, and other land cover types. Emission factors, unique to each of these three land cover types (19, 31), were then used to convert the optimized CO fluxes to total carbon losses (see below). Although carbon emission estimates were obtained from step 1 at a 1° × 1° resolution, they needed further refinement (steps 2–4) because they did not include detailed spatial information about burning in peatlands, forests, and other land cover types and because CO emissions estimates were not based on emission factors specific for peat. In our approach, we accounted for uncertainties associated with the spatial domain of

ENVIRONMENTAL SCIENCES

the optimization (Table S3, see below), emission factors (Table S1 and Table S2), uncertainties in MOPITT observations, and model uncertainties (see below).

MOPITT Optimization. The spatial domain for our regional optimization was chosen on the basis of the highest spatial and temporal correlation of the bottom-up model with MOPITT observations during 2002–2006. This corresponded to regions 3–7 in Table S3 and the scalars that we used to optimize the agreement between the bottom-up model and MOPITT were the mean scalars of these five regions and were applied to the whole study period assuming time independence. We used two different optimization formulations when comparing mean modeled with mean measured column CO mixing ratios for the different box sizes (Table S3). In the first approach, we removed the mean seasonal cycle from both the modeled and the measured CO column time series at each grid cell. This was done because most sources external to the region did not contribute to large interannual variability of atmospheric CO within equatorial Asia (in contrast to the local fire emissions that were the focus of our analysis). We then solved for two scalars (that were applied to the Borneo and Sumatra anomaly time series) to best match observed CO column anomalies. In the second optimization, we adjusted three scalars [Sumatra fire emissions, Borneo fire emissions, and the rest of the world (ROTW), which included fossil fuel emissions, oxidation of CH_4 and Volatile Organic Compounds (VOCs), and contributions from fires outside the study region] to best match the observed CO column absolute values.

These two approaches are referred to as the anomaly and the absolute optimization, respectively. The two optimization approaches provided confidence that the bottom-up model run captured both the temporal variability and the magnitude of the fires in Borneo. Both optimizations indicated that emissions in Sumatra were lower than that predicted by our bottom-up model. This was most apparent in the absolute optimization. Emissions from Sumatra, however, covaried with the influx from fossil fuel emissions from mainland Asia, and, as a result, Sumatra was not as well constrained as Borneo.

In the main text, we present estimates from the anomaly optimization because of the smaller impact of the covariance with fossil fuel emissions transported from mainland Asia. This required a smaller reduction in emissions in Sumatra, which is also physically more plausible because a larger reduction would indicate that emissions per detected fire were much lower in Sumatra than for the better-constrained case of Borneo, even though fire processes and fuel loads were comparable between the two regions. Average fire emissions for Sumatra were 23% lower for the absolute optimization case (Table S4), within the uncertainty range based on the anomaly optimization. Emissions from other islands were too small to be optimized and were combined with emissions from Borneo in both optimization approaches.

Emission Factor Assessment. Emission factors (EFs) were used to translate CO emissions to carbon losses. The amount of CO emitted per unit carbon combusted varies between fires with different types of fuel. We used CO EFs of 210 ± 40, 104 ± 20, and 65 ± 20 g CO per kilogram dry matter burned for peat fires, deforestation fires, and other fires, respectively (19, 31) assuming that biomass was composed of 45% carbon. The EF standard deviations were based on a range of measurements except for tropical peat fires where only one measurement was available (19). The peat EF standard deviation was assumed proportional to the EF for deforestation fires. Some confidence in the peat EF comes from studies in boreal and temperate regions measuring comparable EFs (34). To derive the average EF for the regions on the basis of the fractions of each fire type, we used two scenarios: one where each active fire detected by MODIS represented an equal amount of carbon combusted and one where each detected fire represented an equal amount of area burned (Tables S1 and S2). To convert area burned to emissions we used reported (4) carbon densities of peat and forests, with the depth of burning varying as a function of the number of active fire detections within the same grid cell within one fire season [fire persistence (26, 27)]. Each active fire detected in the same grid cell and year was assumed to burn 10 cm into the peat layer. The 95th percentile of number of persistent fires in the same 1-km area in the study domain was 9. This resulted in a depth of burning of 90 cm in grid cells with high fire persistence, similar to reported maximum depths (4). Because fuel loads per unit area were much higher in peat grid cells than in forest or agriculture grid cells, the combined EF for the scenario where each fire represented an equal amount of area burned was highest (Tables S1 and S2). We used the mean EF of the two scenarios to translate CO emissions into carbon losses, and the standard deviation was taken in quadrature (Tables S1 and S2).

Forest Clearing Rates. Areas of forest loss were determined from yearly composites derived from MODIS 250-m daily imagery with accuracy assessment performed using Landsat data. For 2000 and 2001 we used Terra MODIS imagery for the entire year while for 2002 onward we used both Terra and Aqua MODIS data, but only for the July 1 to December 31 period because this provided sufficient cloud-free observations. We calculated Normalized Difference Vegetation Index (NDVI), taking cloud-free pixels into account only on the basis of blue band reflectance (7) and pixels with view angles $<40°$. For the annual composite the median values of the remaining pixels were selected. The composites were spatially filtered using a 3×3 median filter to remove outliers and data artifacts. Our baseline was areas with $>50\%$ tree cover in 2000 (33). Pixels where NDVI values dropped >0.45 were identified as cleared. This NDVI threshold was determined iteratively on the basis of comparison with high-resolution Landsat data described below. The date of forest loss was estimated as the middle date between detection and last observation. The forest loss event was allocated to the previous year if it was before March 31, the middle month of the wet season (Fig. 4). Accuracy was determined using a coregistered, cloud-masked Landsat 7 ETM pair, path 118, row 061, from July 16, 2000 and February 15, 2003. The difference between the Aerosol-Free Vegetation Index values (AFRI, ref. 35), scaled from 0 to 255, of each scene was calculated, and a threshold of 20 digital numbers was visually selected to determine areas of forest loss. Comparison with MODIS results from March 1, 2002 to February 15, 2003 showed very good agreement of spatial patterns (Fig. S5). Error values were determined after aggregating the Landsat forest loss product to 250-m resolution and removing isolated single pixels from both Landsat and MODIS results, and then buffering at a distance of one 250-m pixel. The omission error was 21.0% and the commission error 23.1%. The accuracy assessment was affected by the uncertainty of exact dates of forest loss in both products and the lack of field data for comparison.

Emissions Uncertainty Assessment. Bottom-up model uncertainties of fire emissions are generally large because of substantial spatial and temporal variability in burned area and fuel loads. By comparing our bottom-up modeled emission estimates with MOPITT retrieved CO, however, the bottom-up model estimates of CO fluxes could be constrained. Remaining uncertainties stem from the partitioning of fire emissions among different land cover types (which is a key uncertainty associated with the EFs that link the CO fluxes back to carbon losses), the spatial domain of the optimization, atmospheric transport and chemistry, and MOPITT observations. Near source regions, MOPITT observations may have dropped out during high fire emissions periods. Our sampling strategy of sampling the model only during times when measurements were available probably reduced the sensitivity of our results to this potential bias. Nevertheless, some errors may have been introduced during the data aggregation and gridding process.

To test how sensitive our results were to the partitioning of fire emissions among land cover types, we used the regional physical planning project for transmigration (RePPProt) peat map to assess in which land cover type fires occurred. This map has more detail than the World Wildlife Fund ecoregions map (32) we used but the spatial extent is limited to Kalimantan. This resulted in a lower share of peat fires and lowered the average EF by 8% and thus increased carbon emissions by 8%, well within our overall uncertainty range.

To determine the standard deviation of our measurements, we used derived standard deviations for EFs, assumed a 10% standard deviation on monthly MOPITT measurements (to cover MOPITT, model, and aggregation errors), which yielded a conservative χ^2 value of 0.36, and used a subjective estimate for the standard deviation for the different spatial domains (Table S3). Standard deviations were propagated through quadrature based on variances to give equal weight to individual errors.

ACKNOWLEDGMENTS. This research was supported by National Aeronautics and Space Administration grants NNG05GD20G, NNG04GK49G, and NNG04GD89G. G.R.v.d.W. was supported by a Veni grant from the Netherlands Organization for Scientific Research.

1. Page SE, *et al.* (2004) A record of Late Pleistocene and Holocene carbon accumulation and climate change from an equatorial peat bog (Kalimantan, Indonesia): implications for past, present and future carbon dynamics. *J Quat Sci* 19:625–635.
2. Rieley JO, Ahmad-Shah AA, Brady MA (1996) *Proceedings of a Workshop on Integrated Planning and Management of Tropical Lowland Peatlands*, eds Maltby E, Immirzi CP, Safford RJ (IUCN, Cambridge, UK), pp. 17–53.
3. Immirzi CP, Maltby E, Clymo RS (1992) *A Report for Friends of the Earth by the Wetland Ecosystems Research Group* (Department of Geography, University of Exeter, Exeter, UK), pp. 1–145.
4. Page SE, *et al.* (2002) The amount of carbon released from peat and forest fires in Indonesia during 1997. *Nature* 420:61–65.
5. Hooijer A, Silvius M, Wösten H, Page S (2006) PEAT-CO2: assessment of CO2 emissions from drained peatlands in SE Asia (Delft Hydraulics, Delft, The Netherlands), report Q3943.

6. Murdiyarso D, *et al.* (2004) Policy responses to complex environmental problems: insights from a science-policy activity on transboundary haze from vegetation fires in Southeast Asia. *Agr Ecosys Environ* 104:47–56.
7. Langner A, Miettinen J, Siegert F (2007) Land cover change 2002–2005 in Borneo and the role of fire derived from MODIS imagery. *Glob Change Biol* 13:2329–2340.
8. Curran LM, *et al.* (2004) Lowland forest loss in protected areas of Indonesian Borneo. *Science* 303:1000–1003.
9. Langenfelds RL, *et al.* (2002) Interannual growth rate variations of atmospheric CO_2 and its $\delta^{13}C$, H_2, CH_4, and CO between 1992 and 1999 linked to biomass burning. *Global Biogeochem Cycles* 16:GB001466.
10. van der Werf GR, *et al.* (2004) Continental-scale partitioning of fire emissions during the 1997 to 2001 El Niño/La Niña period. *Science* 303:73–76.
11. Heil A, Goldammer JG (2001) Smoke-haze pollution: a review of the 1997 episode in Southeast Asia. *Reg Environ Change* 2:24–37.
12. Langmann B, Heil A (2004) Release and dispersion of vegetation and peat fire emissions in the atmosphere over Indonesia 1997/1998. *Atmos Chem Phys* 4:2145–2160.
13. Duncan BN, *et al.* (2003) Indonesian wildfires of 1997: impact on tropospheric chemistry. *J Geophys Res-Atmos* 108:JD003195.
14. Iguchi T, Kozu T, Meneghini R, Awaka J, Okamoto K (2000) Rain-profiling algorithm for the TRMM precipitation radar. *J Appl Meteorol* 39:2038–2052.
15. Giglio L, van der Werf GR, Randerson JT, Collatz GJ, Kasibhatla P (2006) Global estimation of burned area using MODIS active fire observations. *Atmos Chem Phys* 6:957–974.
16. van der Werf GR, *et al.* (2006) Interannual variability in global biomass burning emissions from 1997 to 2004. *Atmos Chem Phys* 6:3423–3441.
17. Bey I, *et al.* (2001) Global modeling of tropospheric chemistry with assimilated meteorology: model description and evaluation. *J Geophys Res-Atmos* 106:23073–23095.
18. Deeter MN, *et al.* (2003) Operational carbon monoxide retrieval algorithm and selected results for the MOPITT instrument. *J Geophys Res-Atmos* 108:JD003186.
19. Christian TJ, *et al.* (2003) Comprehensive laboratory measurements of biomass-burning emissions: 1. Emissions from Indonesian, African, and other fuels. *J Geophys Res-Atmos* 108:JD003704.
20. Giglio L, Descloitres J, Justice CO, Kaufman YJ (2003) An enhanced contextual fire detection algorithm for MODIS. *Rem Sens Environ* 87:273–282.
21. Denman KL, *et al.* (2007) *Climate Change 2007: The Physical Science Basis. Contribution of Working Group I to the Fourth Assessment Report of the Intergovernmental Panel on Climate Change*, eds Solomon S, *et al.* (Cambridge Univ Press, Cambridge, UK, and New York), pp. 499–587.
22. Friedlingstein P, *et al.* (2006) Climate-carbon cycle feedback analysis: results from the C^4MIP model intercomparison. *J Clim* 19:3337–3353.
23. Li WH, *et al.* (2007) Future precipitation changes and their implications for tropical peatlands. *Geophys Res Lett* 34:GL028364.
24. Hansen J, Sato M, Ruedy R, Lo K, Lea DW, *et al.* (2006) Global temperature change. *Proc Natl Acad Sci USA* 103:14288–14293.
25. Murdiyarso D, Lebel L (2007) *Terrestrial Ecosystems in a Changing World*, eds Canadell J, Pataki D, Pitelka L (Springer, New York), pp. 261–271.
26. Giglio L, Csiszar I, Justice CO (2006) Global distribution and seasonality of active fires as observed with the Terra and Aqua Moderate Resolution Imaging Spectroradiometer (MODIS) sensors. *J Geophys Res-Biogeosc* 111:JG000142.
27. Morton DC, *et al.* (2008) Agricultural intensification increases deforestation fire activity in Amazonia. *Glob Change Biol* 14:2262–2275.
28. Casson A (2000) *The Hesitant Boom: Indonesia's Oil Palm Sub-Sector in an Era of Economic Crisis and Political Change* (http://www.cifor.cgiar.org/publications/pdf_files/OccPapers/OP-029.pdf).
29. Marland G, Boden TA, Andres RJ (2007) *Trends: A Compendium of Data on Global Change* (Carbon Dioxide Information Analysis Center, Oak Ridge National Laboratory, U.S. Department of Energy, Oak Ridge, TN) (http://cdiac.esd.ornl.gov/trends/trends.htm).
30. Gullison RE, *et al.* (2007) Tropical forests and climate policy. *Science* 316:985–986.
31. Andreae MO, Merlet P (2001) Emission of trace gases and aerosols from biomass burning. *Glob Biogeochem Cycles* 15:955–966.
32. Olson DM, *et al.* (2001) Terrestrial ecoregions of the world: a mew map of life on Earth. *BioScience* 21:933–938.
33. Hansen MC, Townshend JRG, Defries RS, Carroll M (2005) Estimation of tree cover using MODIS data at global, continental and regional/local scales. *Int J Rem Sens* 26:4359–4380.
34. Yokelson RJ, Susott R, Ward DE, Reardon J, Griffith DWT (1997) Emissions from smoldering combustion of biomass measured by open-path Fourier transform infrared spectroscopy. *J Geophys Res-Atmos* 102:18865–18877.
35. Karnieli A, Kaufman YJ, Remer L, Wald A (2001) AFRI - aerosol free vegetation index. *Rem Sens Environ* 77:10–21.
36. Huffman GJ, *et al.* (1997) The Global Precipitation Climatology Project (GPCP) Combined Precipitation Dataset. *Bull Am Meteorol Soc* 78:5–20.
37. Giglio L, Kendall JD, Mack R (2003) A multi-year active fire dataset for the tropics derived from the TRMM VIRS. *Int J Remote Sens* 24:4505–4525.
38. Arino O, Rosaz J-M, Goloub P (1999) The ATSR World Fire Atlas: a synergy with 'Polder' aerosol products. *Earth Obs Q* 64:1–6.